Journal of Cellular Biochemistry 83:21–32 (2001)

Low-Density Caveolae-Like Membrane From *Xenopus laevis* Oocytes is Enriched in Ras

Susan E. Sadler*

Department of Biological Sciences, University of Denver, University Park, Denver, Colorado 80208

Abstract Detergent-free discontinuous sucrose density gradient centrifugation was used to resolve low- and high-density membrane fractions from *Xenopus laevis* oocytes. Compared to high-density membrane, low-density oocyte membrane is enriched two-fold in cholesterol and highly enriched in ganglioside GM1. Protein immunoblotting of membrane fractions from whole cells with polyclonal anti-human caveolin antibody detected multiple bands, including a distinctive triad with apparent molecular weights of 21, 33, and 48 kDa. To more clearly determine which of these caveolin-like protein(s) is associated with the oocyte plasma membrane, microdissection was used to separate external membrane (cortical preparations containing plasma membrane) from intracellular membrane. Cortical membrane preparations displayed a single 21-kDa caveolin-like protein in low-density membrane. Internal oocyte membrane displayed the higher molecular weight bands of 33 and 48 kDa and a lesser amount of the 21-kDa protein in low-density membrane fractions. Monoclonal anti-human Ras antibody detected a single 23-kDa immunoblot band that is enriched an average of eight-fold in low-density membrane fractions prepared from whole cells. This is the first report of caveolin-associated, low-density membrane in amphibian oocytes, and is consistent with a role for caveolin and caveolae-like microdomains in oocyte signal transduction. J. Cell. Biochem. 83: 21–32, 2001.

Key words: *Xenopus laevis*; oocytes; caveolae; caveolin; low-density membrane; Ras

Caveolae are dynamic membrane microdomains that have been observed to facilitate sorting of surface proteins in a number of cell types. Caveolae or caveolae-like structures apparently act to coordinate and mediate signal transduction or play a role in physiological responses in hormone-sensitive cells. Originally identified by Yamada [1955] and designated 'caveolae intracellularis' (little caves) for their flask-like shapes extending inward from the plasma membrane, caveolae and caveolae-like structures are characterized by distinctive biochemical criteria: resistance to solubility by the detergent Triton X-100, a light buoyant density, and enrichment in glycosphingolipids, cholesterol, and lipid-anchored membrane proteins [for reviews, see Anderson et al., 1992; Anderson, 1998; Okamoto et al., 1998].

A number of techniques have been developed for isolation of caveolae and caveolae-like, low-density membrane (LDM) fractions in the presence or absence of detergent. In detergent-free preparations more than 30 proteins appear to be enriched in caveolae relative to other regions of the plasma membrane [Chang et al., 1994]. These include caveolins (a family of 22-kDa signature proteins named by Rothberg et al. [1992] that often serve as markers for caveolae-like membrane domains), GPI-anchored proteins, Gα and Gβ subunits of heterotrimeric GTP-binding proteins, Ras, Raf-1, Rap1A/B, as well as insulin receptor complex proteins (SOS and Grb2), adenylyl cyclase, and PI3-kinase [Anderson, 1998]. In many cases immunodetection of caveolin marker protein can be used to identify caveolae-like membrane, although caveolin is not detectable in preparations of LDM from some cell types. Caveolin amino acid sequence is highly conserved across species lines. Human caveolin shares 86% sequence homology with the chicken protein with only a single amino acid difference along a long central sequence (amino acids 47–136) [Glenney, 1992]. Four mammalian caveolin gene products

Grant sponsor: NIH; Grant number: 1 R15 GM60922.

*Correspondence to: Susan E. Sadler, Department of Biological Sciences, University of Denver, University Park, Denver, CO 80208. E-mail: ssadler@du.edu

Received 16 February 2001; Accepted 13 April 2001

DOI 10.1002/jcb.1207

have been cloned (caveolin-1α, -1β, -2, and -3), and identification, sequencing, and expression of caveolin-2 defined the caveolin gene family [Scherer et al., 1996].

Ultrastructural analysis of human oocytes, as well as biochemical and pharmacological evidence from the amphibian oocyte system, suggest a possible role for caveolae-like structures in triggering meiotic maturation. Recent structural analysis of human oocytes using transmission electron microscopy has identified pinocytic caveolae on the cell surface [Sathananthan, 1997]. A possible role for caveolae in the amphibian oocyte system can be deduced from previously published biochemical and pharmacological evidence. Amphibian oocytes are physiologically arrested in G2 of meiosis I, and can be induced to mature (reinitiate the meiotic cell cycle) in response to treatment with the presumed natural hormone, progesterone [Masui, 1967], as well as the peptide hormones, insulin, or insulin-like growth factor-1 (IGF-1) [El-Etr et al., 1979; Maller and Koontz, 1981]. Hormone-induced changes in adenylyl cyclase [Finidori-Lepicard et al., 1981; Jordana et al., 1981; Sadler and Maller, 1981] and phosphodiesterase activities [Sadler and Maller, 1987; Sadler, 1991a,b] appear to be responsible at least in part for a decrease in oocyte cAMP that occurs soon after treatment of oocytes with inducing hormone [Maller and Krebs, 1980; Maller, 1985; Smith, 1989]. Inhibition of *Xenopus* oocyte adenylyl cyclase by progesterone shares features with P-site as well as receptor-mediated mechanisms [Sadler and Maller, 1983]. More recently, there has been some speculation that P site adenosine action may be associated with caveolae [Anderson, 1993]. It is conceivable that the steroid hormone-sensitive G protein signal transduction system and the P site-like effects of progesterone in amphibian oocytes may be localized to caveolae-like membrane microdomains. It is also intriguing to speculate that growth-promoting peptide hormone action may involve caveolae. Analysis of insulin- and IGF-1-binding, internalization, and induction of oocyte maturation [Taghon and Sadler, 1994] suggests that both insulin and IGF-1 bind to IGF-1 receptors on the amphibian oocyte surface, and that there is a necessary role for receptor-mediated endocytosis in the IGF-1-induced oocyte maturation response. In mammalian cells adipocytes [Goldberg et al., 1987], 3T3-L1 cells [Smith and Jarrett, 1988], H35 hepatoma cells [Smith and Jarrett, 1990], insulin receptor internalization is predominately mediated via caveolae. By analogy, insulin- and IGF-1-signal transduction in amphibian oocytes may also involve caveolae-like structures.

Hormone-induced changes in metabolic processing of membrane phospholipids with coincident changes in oocyte membrane fluidity may also contribute to the molecular cascade that triggers amphibian oocyte meiotic maturation [for review, see Morrill and Kostellow, 1999]. Within seconds of treating *Rana pipiens* oocytes with progesterone, successive waves of 1,2-diacylglycerol (DAG) were produced that are both necessary and sufficient to induce resumption of meiotic cell division. These DAG waves are generated by initial transmethylation of one or more phosphatidylethanolamine pool in the oocyte plasma membrane [Chien et al., 1986], and application of the first product of lipid methylation (phosphatidyl-N-monomethylethanolamine) to oocytes is sufficient to induce nuclear envelope breakdown. The progesterone-induced increase in methyltransferase I activity is followed by an increase in sphingomyelin synthesis that coincides with a decrease in ceramide, thus indicating that the end product of N-methylation undergoes a transfer reaction with ceramide to form sphingomyelin [Morrill et al., 1994]. Strum et al. [1995] demonstrated the necessary role for a sphingomyelin cycle in the *Xenopus* oocyte signal transduction pathway activated by progesterone. De Smedt et al. [1995] reported that an inhibitor of glucosylceramide synthase in the pre-Golgi apparatus was able to increase ceramide in *Xenopus* oocytes to levels that are sufficient to induce meiotic maturation. Morrill's group has also measured progesterone-induced changes in *Rana* oocyte membrane fluidity using electron spin resonance [Morrill et al., 1989]. Progesterone induces a transient dose-dependent decrease in oocyte membrane fluidity (an increase in order parameter) near the membrane surface that correlates with the initial transient increase in phospholipid methylation. Additional work revealed that specific and saturable association of cAMP and a photoaffinity cAMP analog with the cytoplasmic face of prophase arrested *Rana* oocytes increases membrane fluidity, blocks progesterone-induced decreases in membrane fluidity, and inhibits the steroid-induced meiotic res-

ponse [Morrill et al., 1993]. These results further suggest that a change in membrane order is essential for resumption of meiotic division. Hormone-induced changes in membrane order parameters are also compatible with possible involvement of caveolae-like structures in the signal transduction mechanism.

The work reported here was undertaken to test for the presence of caveolae-like, LDM in *Xenopus laevis* oocytes using detergent-free, discontinuous sucrose density gradient centrifugation to separate LDM from high density membrane (HDM). Levels of cholesterol and ganglioside GM1 in oocyte LDM and HDM were compared. Protein immunoblotting was used to test for caveolin-like proteins in membrane fractions prepared from whole cells, plasma membrane-containing cortices, and intracelluar membrane samples. And relative levels of immunodetectable Ras in oocyte LDM and HDM were determined.

METHODS

Experimental Animals and Oocyte Isolation

Mature *Xenopus laevis* females (Xenopus I, Ann Arbor, MI) were housed in aquatic tanks in a temperature-controlled room (16°C) in daily cycles of 14 h light and 10 h dark. Animals were fed diced beef heart twice each week. Frogs were primed by injection of 35 IU of pregnant mare serum gonadotropin (Calbiochem, La Jolla, CA) into the dorsal lymph sac three to seven days before surgical removal of ovary. Ovarian fragments were surgically removed after the frog was anesthetized by immersion in 200 ml of solution containing 0.12% tricaine (3-aminobenzoic acid ethyl ester, Sigma, St. Louis, MO) and 25 mM HEPES (Calbiochem), pH 7.0. Pieces of ovary were stored at room temperature in oocyte ringers containing 83 mM NaCl, 1 mM KCl, 1 mM $MgCl_2$, 0.5 mM $CaCl_2$, 10 mM HEPES, pH 7.9). Individual oocytes [stage VI, according to Dumont, 1972] were manually dissected using watchmaker's forceps under a stereomicroscope and stored in oocyte ringers at room temperature until membrane preparation.

Membrane Preparation and Sucrose Gradient Centrifugation

Manually dissected ocytes, isolated cortices containing plasma membrane [prepared as described in Sadler and Maller, 1981], or internal membrane samples (remaining after cortical removal) were used as starting material for preparation of LDM and high-density membrane (HDM) fractions using a detergent-free method modified from Song et al. [1996a]. Cortices were isolated by piercing, opening, and flattening groups of oocytes under a stereomicroscope with watchmaker's forceps in ice-cold isolation buffer (10 mM NaCl, 10 mM HEPES, pH 7.9). After soaking for 10–20 min, the plasma membrane/vitelline envelope complex (cortex) begins to lift away from the bulk of cellular contents, and the cortices are peeled away from the yolk and intracellular contents with watchmaker's forceps, transferred to and washed in fresh ice-cold isolation buffer using a Pasteur pipette, and collected by microcentrifugation (15,000*g* for 5 min at 4°C). Samples of intracellular membrane were prepared by collecting the cellular debris by microcentrifugation (15,000*g* for 10 min at 4°C) after external membrane had been peeled away. Samples of oocytes or membranes were homogenized in 2 ml of 500 mM sodium carbonate, pH 11.0, containing 10 μg/ml aprotinin, 20 μg/ml leupeptin, 1 mM phenylmethylsulfonyl fluoride, and 50 μM Na-orthovanadate with 40 strokes of a Dounce homogenizer using a loose pestle. The suspension was centrifuged (1,000*g* for 15 min at 4°C) to pellet yolk platelets. After transferring supernatants to fresh tubes, a few drops of homogenization buffer were added to restore 2-ml volumes, and the samples were sonicated using a Fisher Sonic Dismembrator Model 300 (3×20 sec bursts at 30% power). Samples were adjusted to 45% sucrose by addition of 2 ml of 90% sucrose in MBS (MES-buffered saline containing 25 mM MES, pH 6.5, and 150 mM NaCl). These 4-ml mixtures were placed in the bottom of Ultra-Clear centrifuge tubes (Beckman, 14×89 mm), overlaid with 4 ml of 35% sucrose in MBS plus 250 mM Na-carbonate, then 4 ml of 5% sucrose in MBS plus 250 mM Na-carbonate. After overnight ultracentrifugation (15–17 h) in an SW41 Beckman swinging bucket rotor at 39,000 rpm in a Beckman L7 Ultracentrifuge, 1-ml fractions were collected from the top of each tube using a Brandel fractionator with a UV flow cell detector (ISCO, Lincoln, NE). These 1-ml fractions were diluted by addition of 2 ml of MBS, and membrane pellets were collected by centrifugation (15,000*g* for 15 min at 4°C). Membrane pellets

were either resuspended in electrophoresis buffer or extracted with isopropanol for cholesterol measurements.

Protein Immunoblotting

Proteins contained in sucrose gradient fractions were resolved by SDS–polyacrylamide gel electrophoresis (PAGE) [12.5% acrylamide by the method of Laemmli, 1970] before semi-dry electroblot transfer to PVDF membrane (Immobilon-P, Millipore, Bedford, MA) using a Trans-Blot SD apparatus (BioRad, Hercules, CA). After electroblot transfer (0.8 mA/cm^2 of membrane area for 75 min) using electrode solution containing 39 mM glycine, 48 mM Tris, 0.0375% SDS and 20% spectrophotometric grade methanol, the blot was stained with 0.1% Ponceau S in 5% acetic acid to visualize proteins or probed with antibodies to detect caveolin- or Ras-like proteins. A 0.2% solution (weight/volume) of I-Block (Tropix, Bedford, MA) in TBS (150 mM NaCl, 10 mM Tris-HCl, pH 7.5) plus 0.1% Tween-20 was used as blocking agent with overnight rotation at 4°C. Caveolin-like proteins were detected using a 1/2,500 dilution of anti-human caveolin polyclonal antibody (Transduction Laboratories, Lexington, KY) in blocking agent as primary antibody and a 1/2,500 dilution of goat anti-rabbit alkaline phosphatase conjugate (Tropix) in blocking agent as secondary antibody. Ras protein was detected using a 1/500 dilution of anti-human Ras monoclonal antibody (Transduction Laboratories) in blocking agent as primary antibody and a 1/2,500 dilution of goat-anti-mouse alkaline phosphatase conjugate (Tropix) in blocking agent as secondary antibody. Immunoreactive bands were visualized using the CDP-Star detection system (Tropix) with exposure to Fuji RX film.

GM1 Detection

Relative amounts of ganglioside GM1 contained in sucrose gradient fractions were determined using a method modified from Wu et al. [1997]. After dilution in MBS, a 125-μl sample of each sucrose gradient fraction (containing membrane from 8.3 oocyte equivalents) was mixed with 12.5 μl of 1 M NaOH (to yield a 0.1 N NaOH mixture) and was applied to nitrocellulose membrane (BioRad, previously soaked in TBS plus 0.1% bovine serum albumin (TBS/BSA) for 30 min at room temperature) using a Bio-Dot SF slot blot apparatus (BioRad) under gentle aspiration. After slot-blot transfer, the membrane was incubated in a 1/40,000 dilution of 5 mg/ml cholera toxin conjugated to HRP (Sigma), then washed in TBS/BSA (5 × 5 min in 30 ml) and HRP detection buffer containing 500 mM NaCl and 20 mM Tris-HCl, pH 7.5, at room temperature (2 × 5 min in 30 ml). Relative amounts of GM1 were detected by chemiluminescence using SuperSignal (Pierce, Rockford, IL) with exposure to Fuji RX film.

Cholesterol Assay

Cholesterol measurements were made using a modification of the method of Heider and Boyett [1978]. According to Chang et al. [1992] combined membrane pellets from LDM- and HDM-containing sucrose gradient fractions were extracted with isopropyl alcohol (0.3 ml) and the samples were sonicated (3 × 30 sec bursts using a Fisher Sonic Dismembrator Model 300 at 30% power). After centrifugation (800*g* for 15 min), the clear supernatant was transferred to a clean tube. The residue pellet was dissolved in 0.1 N NaOH and used for protein determination. Isopropyl alcoholic solutions of standards, samples and blank (alcohol alone) were used in a spectrophotometric enzyme-linked assay for total cholesterol as follows. A 2-ml aliquot of Reagent A (0.05 M sodium phosphate buffer, pH 7.0, 0.16 U/ml cholesterol ester hydrolase, 0.08 U/ml cholesterol oxidase, 30 U/ml horseradish peroxidase, 5 mM sodium taurocholate, 0.08% Triton X-100, and 0.125 mg/ml *o*-dianisodine) was combined with 200 μl of isopropyl alcohol extract (or standard solution) in a 10 × 75 mm disposable glass tube. The mixtures were incubated at 37°C for 20 min in a shaking heater block, and absorbance at 450 nm was used to determine cholesterol content by comparison to a standard curve. Using this protocol, colorimetric detection was linearly proportional to cholesterol content in the range of 0.5 to 50 nmoles (data not shown).

Data Presentation

Numeric data were plotted using SigmaPlot 4.0 (Jandel Scientific). Digitally scanned images of gels and autoradiographic images of immunoblots and slot blots were formatted and reproduced using PowerPoint (Microsoft Office 97).

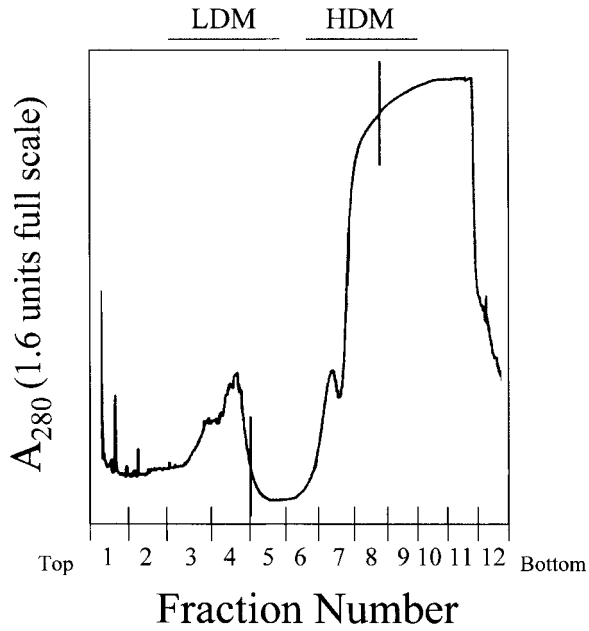

Fig. 1. A_{280} profile of oocyte membrane resolved by discontinuous sucrose gradient centrifugation. A group of 200 oocytes was homogenized and subjected to discontinuous sucrose gradient centrifugation as described in Methods. After ultracentrifugation, relative absorbance at 280 nm was recorded during fraction collection from the top of the centrifuge tube. The absorbance profile is plotted as absorbance at 280 nm (A_{280}) as a function of sample fraction number. After sample dilution and centrifugation, LDM pellets were visible in fractions 3, 4, and 5, and HDM pellets were visible in samples 7, 8, and 9.

RESULTS

After ultracentrifugation on 5–35–45% discontinuous sucrose gradients, oocyte samples prepared in detergent-free Na-carbonate buffer yielded a visible, flocky LDM band above the 5–35% interface and a visible, HDM band above the 35–45% interface. The 45% sucrose portion of the gradient was always discolored with greenish pigmentation. A representative A_{280} profile for gradient fractions collected from the top of the gradient tube is shown in Figure 1. The first peak of optical absorbance (samples 3, 4, and 5) corresponds with visible LDM pellets that were subsequently collected from these samples. The absorbance shoulder (fraction 7) to the left of the major absorbance plateau corresponds to visible HDM pellets that were collected in fractions 7, 8, and 9. The strong absorbance plateau that extends to the bottom of the tube corresponds to the heavily pigmented 45% sucrose cushion at the bottom of the tube.

Coomassie staining of proteins contained in sucrose gradient fractions (Fig. 2, upper panel) demonstrated a fairly even distribution of membrane protein between oocyte LDM (fractions 3, 4, and 5) and HDM (fractions 7, 8, and 9). Ponceau S staining of proteins after electroblot transfer to PVDF membrane demonstrated that 75 min is sufficient to transfer a significant portion of LDM and HDM proteins to the immunoblot membrane (Fig. 2, lower panel).

One distinguishing characteristic of caveolae-like, LDM in other cell systems is its relative enrichment in cholesterol. Total cholesterol and protein content in combined LDM and HDM membrane samples from 200 oocytes removed from two different donor animals were measured and compared (Table I). When values for the two sample sets were averaged ($n = 2$, ±half-range), combined LDM fractions contained 28±2 μg of protein and HDM fractions contained 22±2 μg of protein. These values substantiate the apparent even distribution of membrane protein between LDM and HDM observed with Coomassie staining in Figure 1. When cholesterol content is expressed per microgram of protein, LDM contains 0.38±0.03 nmol cholesterol/μg protein and HDM contains 0.19±0.01 nmol cholesterol/μg protein. Therefore, LDM prepared from whole oocytes is approximately two-fold enriched in cholesterol compared to HDM.

In many other cell types caveolin is the signature protein marker for low-density caveolae-like membrane. As shown in Figure 3, when sucrose gradient fractions from whole oocytes are immunoblotted with anti-caveolin antibody, a triad of three distinctive protein bands is evident in LDM-containing fractions 4 and 5. These caveolin-like bands have apparent molecular weights of 21, 33, and 48 kDa. Although of lesser intensities, the higher molecular weight bands (33-, and 48-kDa) are also evident in HDM membrane fractions 8 and 9. Other minor immunoblot bands are also evident on some immunoblots with longer film exposure. The specificity of the anti-caveolin antibody binding is demonstrated by comparison of the anti-caveolin blot (Fig. 3, upper panel) to a companion immunoblot probed with normal rabbit serum in place of primary antibody (Fig. 3, lower panel). When the immunoblot band pattern for LDM fractions from oocytes was compared to the immunoblot band pattern for human endothelium (the control extract provided by

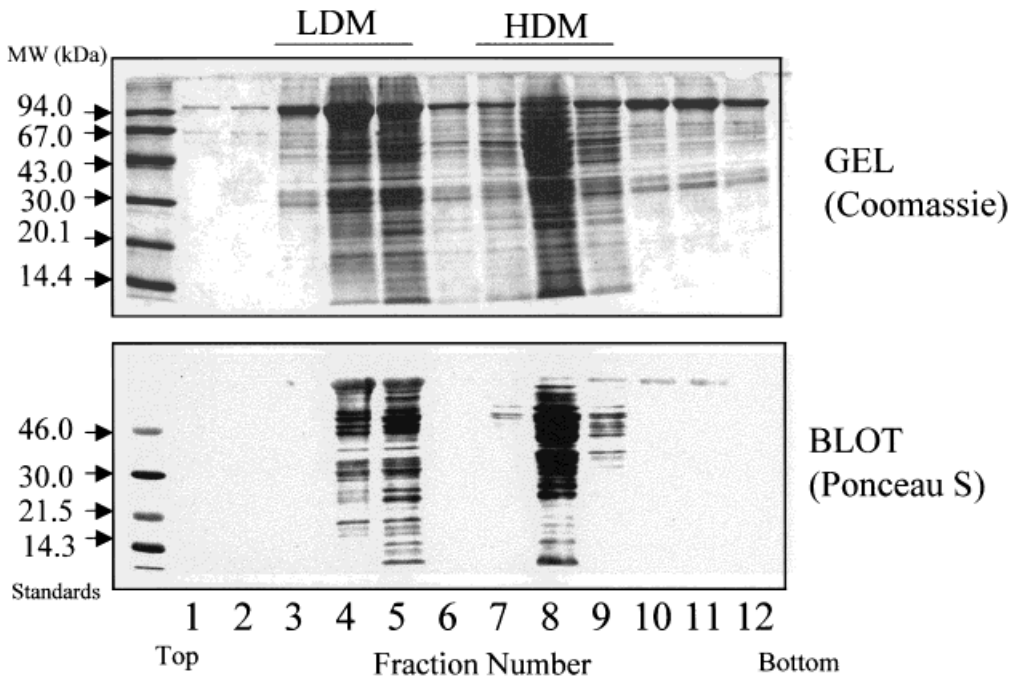

Fig. 2. Electrophoretic profiles of proteins contained in sucrose gradient fractions. After resolution of sucrose gradient fractions containing membrane from 100 oocytes by SDS–PAGE on a 12.5% acrylamide gel, proteins in the gel were visualized by standard Coomassie staining (upper panel, GEL (Coomassie)). A companion gel was electroblot transferred to PVDF membrane and visualized by staining with 0.1% Ponceau S in 5% acetic acid (lower panel, BLOT (Ponceau S)). Numbers to the left of each panel indicate the apparent molecular weights of commercial standards that were resolved in the left lane of each panel (upper panel: unstained markers (Pharmacia); lower panel: prestained markers (BioRad)).

the antibody supplier, Transduction Laboratories), the 21-kDa oocyte band lined up with a band in the human endothelium sample that is just below the major 22.5-kDa band (data not shown).

Since oocytes contain extensive intracellular membrane, and since the relatively equal amounts of LDM and HDM protein isolated from oocytes contrasts with the relatively unequal amounts of LDM and HDM observed in most other cell types (see discussion), it was of interest to compare the LDM and HDM protein profiles in manually isolated external membrane (cortices that contain plasma membrane) to the LDM and HDM protein profiles in internal membrane. Cortices were manually dissected as described in Methods, and residual internal cellular content was collected. Figure 4 shows the silver stained protein patterns in polyacrylamide gels of sucrose density gradient fractions from these two starting preparations. Both gels in Figure 4 were developed for equal

TABLE I. Total Cholesterol Levels Measured in LDM and HDM Samples

Donor animal	Membrane fraction	Cholesterol (nmoles)	Protein (μg)	nmol cholesterol/ μg protein
A	LDM	12.3	30	0.41
B	LDM	9.6	27	0.36
A	HDM	4.8	24	0.20
B	HDM	3.7	20	0.19

Two sets of 800 oocytes were isolated from different donor animals (A and B), and fractions containing LDM and HDM were resolved by discontinuous sucrose gradient centrifugation. After collection of gradient fractions, samples from each set containing LDM (gradient fractions 3, 4, and 5) were combined, and samples containing HDM (gradient fractions 7, 8, and 9) were combined. Pooled samples were collected by centrifugation and resuspended in MBS. An aliquot of each (containing a 200 oocyte equivalent) was extracted with isopropanol. As described in Methods, levels of total cholesterol were measured using an enzyme-linked assay. For calculation of "specific" cholesterol (nmol of cholesterol/μg of protein) the protein contained in the residual pellet after cholesterol extraction was resuspended in 0.1 M NaOH, and protein content was determined using the Lowry method.

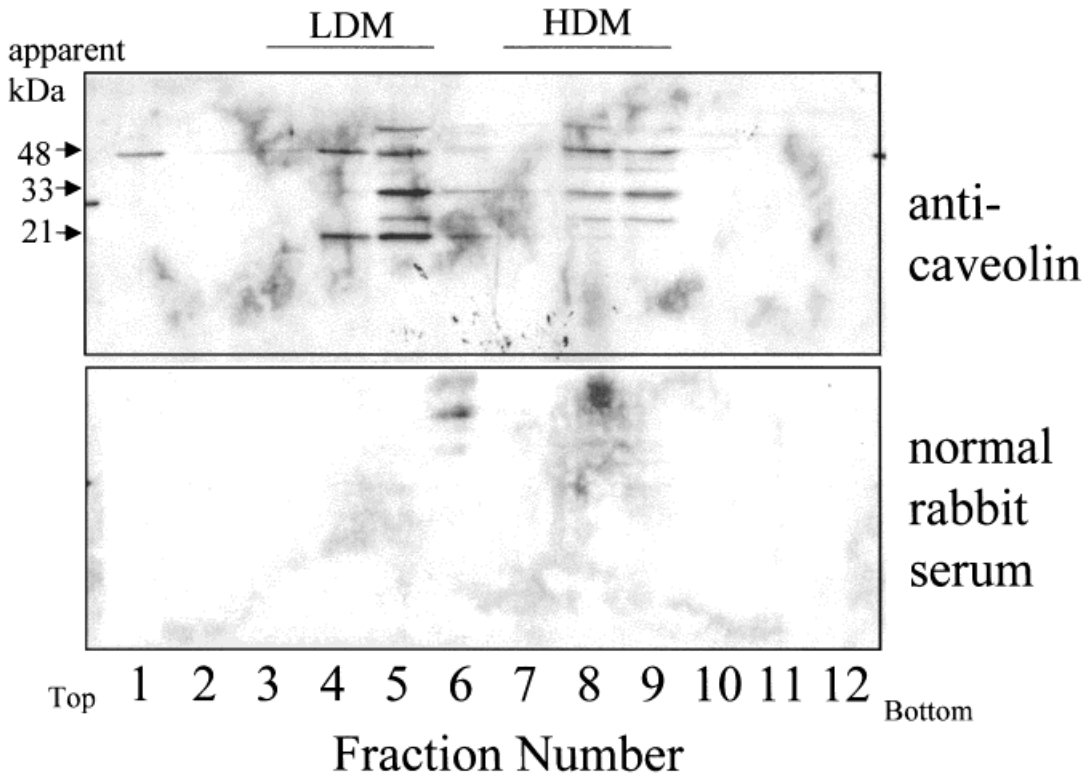

Fig. 3. Immunoblot detection of caveolin-like proteins in membrane fractions. Following separation by discontinuous sucrose gradient centrifugation, proteins contained in gradient fractions from membranes from 100 oocytes were resolved by SDS–polyacrylamide electrophoresis, electroblot transferred to PVDF membrane, and detected using a 1/2,500 dilution of polyclonal rabbit anti-human caveolin (upper panel) or normal rabbit serum (lower panel). Secondary antibody for each was a 1/2,500 dilution of goat anti-rabbit conjugated to alkaline phosphatase. The chemiluminescent image was generated using CDP Star and 5 min exposure to Fuji RX film. Numbers to the left of the upper panel indicate the apparent molecular weights of the triad of major detectable bands (determined by comparison to the relative migration of prestained low molecular standards, BioRad).

time (8 min using BioRad SilverStain Plus). This development time was sufficient to visualize the protein pattern in the cortical preparation (Fig. 4, lower panel) but resulted in very heavy staining of the internal membrane gradient fractions (Fig. 4, upper panel). In contrast to the relatively equal amounts of protein in HDM (lanes 7, 8, and 9) and LDM (lanes 3, 4, and 5) from internal membrane (Fig. 4, upper panel), HDM from oocyte cortices contains significantly more silver-stained protein than cortical membrane LDM (Fig. 4, lower panel).

It was of interest to determine whether the oocyte caveolin-like proteins are associated with plasma membrane or cytosolic membrane. As described in Methods, oocyte cortices (containing plasma membrane associated with vitelline envelope) were manually dissected away from internal membrane and yolk, LDM and HDM were resolved, and LDM gradient fractions were resolved by electrophoresis and probed with anti-caveolin antibody. As shown in Figure 5, the 21-kDa caveolin-like band was detected in LDM from cortical membrane samples (cortices, fractions 4 and 5). The higher molecular weight caveolin-like bands are contained in internal membrane (fractions 4, 5, and 6). When a full gradient profile was probed with anti-caveolin antibody, the 21-kDa caveolin-like band was detected only in cortical LDM fractions and was not detected in cortical HDM fractions (data not shown). When cortices are manually peeled away from cellular debris, the majority of pigment granules are left behind, suggesting minimal cytosolic membrane contamination of cortical membrane preparations. But sometimes cortices tear as they are pulled away. Samples of internal membrane may be contaminated with small fragments of plasma membrane. It remains to be determined whether or not the faint 21-kDa band in internal membrane LDM fraction 4 (Fig. 5) reflects

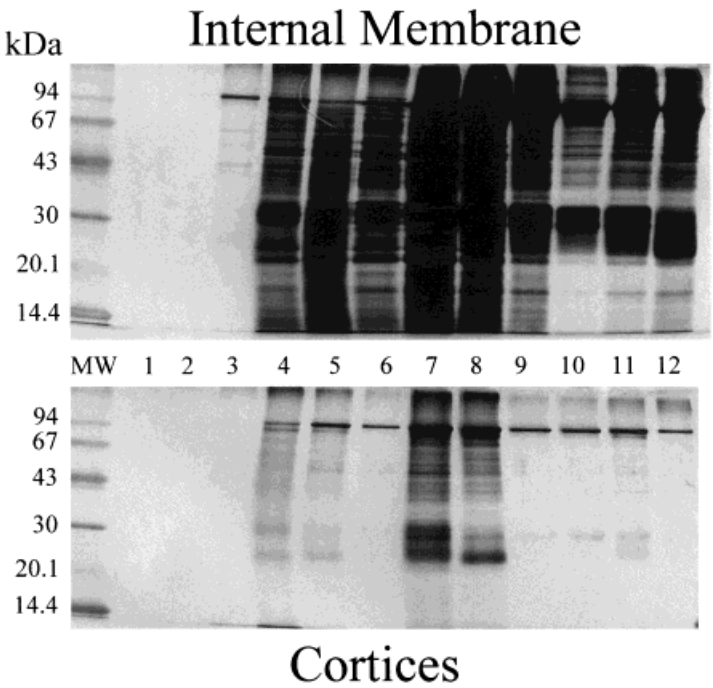

Fig. 4. Silver stained electrophoretic profiles of proteins resolved from external and internal membrane. External cortices (containing plasma membrane) were manually separated from internal membrane before homogenization and sucrose gradient centrifugation, as described in Methods. Proteins in gradient fractions (1–12) collected from the equivalent of 100 oocyte cortical membranes (lower panel) or internal membrane from 100 oocytes (upper panel) were resolved by SDS–PAGE and stained with BioRad Silver Stain Plus according to the manufacturer's instructions (8 min development reaction). The left lane in each panel contains commercial low molecular weight standards (Pharmacia), and apparent molecular weights for standard proteins are shown by the numbers to the left.

contamination of internal membrane samples with plasma membrane or 21-kDa caveolin-like protein associated with cytosolic membrane.

In addition to relative enrichment in cholesterol content, another distinguishing feature of caveolae-like membranes in other cell systems is that they are also enriched in ganglioside GM1. Therefore, it was of interest to compare relative levels of ganglioside GM1 contained in sucrose gradient fractions from whole cells and cortices. Slot blots of membrane fractions were evaluated using horseradish peroxidase-conjugated cholera toxin (as described in Methods). When whole oocytes were used as starting material, the LDM fractions (Fig. 6, upper panel, fractions 3, 4, and 5) were enriched in

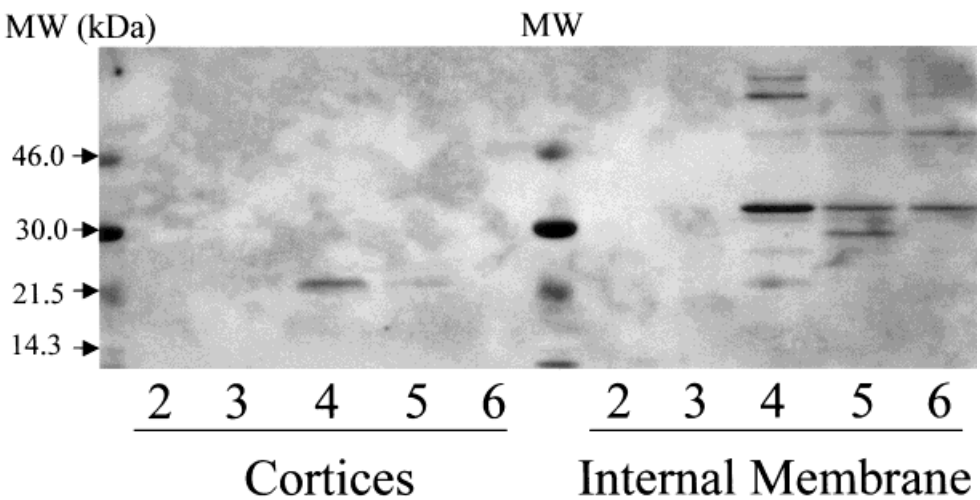

Fig. 5. Immunoblot detection of caveolin-like proteins in LDM fractions from external and internal membrane. After manual separation of plasma membrane-containing cortices from internal membrane stores (100 oocytes), proteins contained in gradient fractions 2, 3, 4, 5, and 6 were resolved by SDS–PAGE (12.5% acrylamide) and detected by immunoblotting using anti-human caveolin antibody. Numbers to the left indicate the apparent molecular weights of pre-stained molecular weight standards (BioRad) in the left and middle lanes (MW).

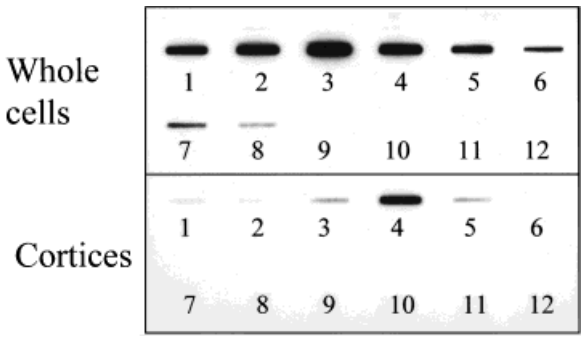

Fig. 6. Slot blot detection of ganglioside GM1 contained in gradient fractions. Samples of sucrose gradient fractions (1–12) that were prepared using whole cells (upper panel) or external membrane cortices (lower panel) as starting material were treated with 0.1 N NaOH (by addition of 1/10 volume of 1 N NaOH) and applied by vacuum aspiration to nitrocellulose membrane. The slot blot was probed with a 1/40,000 dilution of 5 mg/ml cholera toxin-horse radish peroxidase conjugate and detected by chemiluminescence.

GM1 compared to HDM (fractions 7, 8, and 9), but ganglioside GM1 was also detected at significant levels in fractions at the top of the gradient. It is interesting that the largest amount of ganglioside GM1 was detected in fraction 3 (Fig. 6, upper panel) at the leading edge (on the more buoyant side) of visible LDM membrane pellets (fractions 3, 4, and 5). When oocyte cortices containing plasma membrane were used as starting material, ganglioside GM1 was detected more cleanly in gradient fractions 3, 4, and 5 (the LDM fractions that yield visible membrane pellets) with the greatest level in fraction 4 (Fig. 6, lower panel). Thus, LDM from amphibian oocytes is also highly enriched in ganglioside GM1.

Finally, protein immunoblotting was used to compare relative levels of Ras protein associated with oocyte LDM and HDM. As shown in Figure 7, a single 23-kDa band was detected with monoclonal anti-Ras antibody. LDM fractions 4 and 5 contain the largest amount of Ras, and oocyte LDM is apparently enriched in Ras compared to oocyte HDM (compare fractions 3, 4, and 5 to fractions 7, 8, and 9). Linear spectrophotometric scanning of anti-Ras immunoblot bands was used to quantify the relative amounts of Ras in LDM and HDM. When data from three blots using samples from oocytes collected from three different donor females were analyzed and compared, the relative densities in combined LDM lanes ranged from 5- to 13-times higher than the relative densities of anti-Ras bands in the combined HDM lanes (data not shown). In these three experiments Ras was enriched at least five-fold (an average of eight-fold) in LDM compared to HDM.

DISCUSSION

The biochemical and immunoblot data presented here are the first to substantiate the presence of low-density caveolae-like membrane in amphibian oocytes. Certain features of the amphibian oocyte caveolae-like membrane are very similar to caveolae-like membrane in mammalian cells, and certain differences are noteworthy.

Sucrose gradient fractionation of mammalian tissue prepared in the presence or absence of detergent generally yields a protein profile in which the majority of protein is contained in HDM fractions with very little protein contained in LDM fractions. Unlike the staining profile of oocyte membrane (Fig. 2) in which almost equal amounts of stainable protein are contained in LDM and HDM fractions, detergent preparations from MDCK cells [Tang et al., 1996], and non-detergent preparations from differentiated C2C12 skeletal myoblasts [Song et al., 1996b] or cultured human fibroblasts

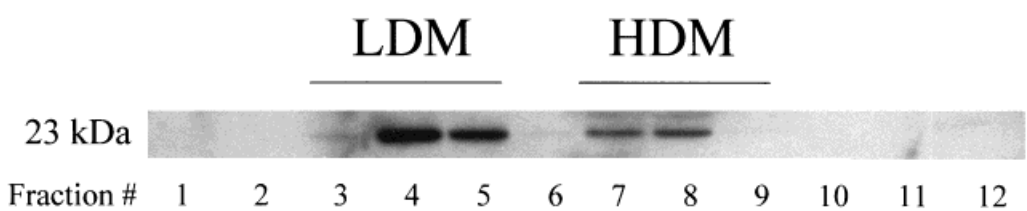

Fig. 7. Immunoblot detection of Ras protein in LDM and HDM fractions. Sucrose gradient fractions (1–12) were prepared from whole oocytes, resolved by SDS–PAGE, and analyzed by protein immunoblotting using a 1/500 dilution of monoclonal anti-Ras with chemiluminescent detection. A single 23-kDa band was detected. Linear scanning of the bands in this immunoblot indicated that the LDM (lanes 3, 4, and 5 combined) are approximately five-fold enriched in Ras compared to HDM (lanes 7, 8, and 9 combined).

[Smart et al., 1995] displayed levels of LDM so low that they were not detected with Ponceau S staining of the immunoblot membrane. When external cortices, containing plasma membrane, were pulled away from internal oocyte membrane stores, it was evident that the bulk of the oocyte LDM is contained in internal membrane stores (Fig. 4). The profile of silver staining for cortices (Fig. 4, lower panel) is more similar to previously published mammalian tissue profiles, with the majority of protein contained in HDM fractions and less protein contained in the LDM fractions.

Relative enrichment of oocyte LDM in cholesterol (Table I) and ganglioside GM1 (Fig. 6) is similar to that observed in mammalian cells. Smart et al. [1995] reported that cholesterol is six-fold enriched in caveolae from MA104 monkey kidney epithelial cells. LDM from oocytes is at least two-fold enriched in cholesterol (Table I). This value was calculated based upon the protein measured in combined membrane pellets from whole oocytes in which protein content in LDM and HDM is similar (Table I). Since relative protein content between LDM and HDM in oocyte external membrane is very different, with LDM containing much less protein than HDM fractions (as evidenced by silver staining in Fig. 4), the "specific" cholesterol value calculated using protein contained in pooled membrane may underestimate the relative enrichment in LDM fractions in the oocyte plasma membrane. A more sensitive cholesterol assay is needed in order to reliably measure cholesterol content in isolated cortices. Nonetheless, like mammalian caveolae-like membrane, amphibian oocyte LDM is also enriched in cholesterol and ganglioside GM1.

In contrast to many published reports of caveolin profiles in mammalian cells, polyclonal anti-human caveolin antibody detects a prominent triad of immunoblot bands in amphibian oocyte preparations. A 21-kDa band is enriched in LDM fractions from plasma membrane compared to internal membranes (Fig. 5), but is not detected in HDM fractions from whole cells (Fig. 3). Similar to caveolae-like membrane in many mammalian cell types, LDM from amphibian oocytes also contains a single caveolin-like marker protein (Fig. 5). Higher molecular weight (33- and 48-kDa) immunoblot bands are contained in LDM fractions from intracellular membrane stores (Fig. 5). It is not clear whether these higher molecular weight immunoreactive bands indicate different amphibian caveolin-like proteins, precursor proteins that are being processed in intracellular membrane, cross-reaction with non-caveolin proteins, or the existence of caveolin hetero- or homodimers. Further experimentation is needed to investigate these possibilities.

Dynamic interactions of signaling proteins, including Ras, with caveolae-like membrane domains in mammalian cells has led to formulation of a working model in which caveolae function as signaling depots in certain cells. Ras is detected in caveolae of EGF-sensitive normal Rat-1 cells [Mineo et al., 1996], and is enriched in caveolae-like domains from neuronal plasma membrane prepared from rat forebrain synaptic plasma membrane [Wu et al., 1997]. Deletion analysis has shown that Ras binding is localized to a 41-amino acid region of the cytosolic N-terminal domain of caveolin [Song et al., 1996a]. Since Ras is also concentrated in oocyte LDM (Fig. 5) which contains the putative amphibian caveolin marker protein (Fig. 5, cortical fractions 3, 4, and 5), caveolae-like structures may also play a dynamic role in modulating the interplay of signaling proteins during induction of the oocyte maturation response. However, it is important to realize that LDM fractions prepared by nonspecific physical techniques, like the sucrose gradient technique used in this study, have been reported to be heterogeneous in vesicular and membrane content [Stan et al., 1997], and the presence of signaling proteins in caveolae remains controversial. There may exist cell- and tissue-specific differences in caveolae function in hormone-sensitive and hormone-insensitive cells. Nonetheless, the data presented here are consistent with a possible role for caveolae-like structures in amphibian oocytes. Continuing experimentation will investigate this hypothesis.

In summary, data presented here offer the first experimental evidence for caveolae-like, LDM in amphibian oocytes. Analogous to mammalian cells, the amphibian LDM is enriched in cholesterol and ganglioside GM1. Cortical membrane (containing plasma membrane) displays a 21-kDa protein that is detected with anti-human caveolin polyclonal antibody. Internal oocyte membrane apparently contains a lesser amount of the 21-kDa protein and higher molecular weight caveolin-like proteins. Thus, a caveolin-like protein is

associated with amphibian low-density, caveolae-like membrane on the oocyte surface. Localization of *ras* protein to these low density fractions suggests that caveolae-like structures may play a role in organizing signal transduction proteins that trigger the hormone response in the amphibian oocyte system.

Preliminary results were presented as a poster at the American Society for Cell Biology, December, 2000 [Sadler, 2000].

REFERENCES

Anderson RGW. 1993. Caveolae: where incoming and outgoing messengers meet. Proc Natl Acad Sci 90: 10909–10913.

Anderson RGW. 1998. The caveolae membrane system. Annu Rev Biochem 67:199–225.

Anderson RGW, Kamen BA, Rothberg KG, Lacy SW. 1992. Potocytosis: sequestration and transport of small molecules by caveolae. Science 255:410–411.

Chang WJ, Rothberg KG, Kamen BA, Anderson RGW. 1992. Lowering the cholesterol content of MA104 cells inhibits receptor-mediated transport of folate. J Cell Biol 118:63–69.

Chang WJ, Ying YS, Rothberg KG, Hooper NM, Turner AJ, Gambliel HA, DeGunzburg J, Mumby SM, Gilman AG, Anderson RGW. 1994. Purification and characterization of smooth muscle cell caveolae. J Cell Biol 126:127–138.

Chien EJ, Kostellow AB, Morrill GA. 1986. Progesterone induction of phospholipid methylation and arachidonic acid turnover during the first meiotic division in amphibian oocytes. Life Sci 39:1501–1508.

De Smedt V, Rime H, Jessus C, Ozon R. 1995. Inhibition of glycosphingolipid synthesis induces $p34^{cdc2}$ activation in *Xenopus* oocyte. FEBS Lett 375:249–253.

Dumont JN. 1972. Oogenesis in *Xenopus laevis* (Daudin). I. Stages of oocyte development in laboratory maintained animals. J Morph 136:153–180.

El-Etr M, Schorderet-Slatkine S, Baulieu EE. 1979. Meiotic maturation in *Xenopus laevis* oocytes initiated by insulin. Science 205:1397–1400.

Finidori-Lepicard J, Schorderet-Slatkine S, Hanoune J, Baulieu EE. 1981. Progesterone inhibits membrane-bound adenylate cyclase in *Xenopus laevis* oocytes. Nature 292:255–257.

Glenney JR Jr. 1992. The sequence of human caveolin reveals identity with VIP21, a component of transport vesicles. FEBS Lett 314:45–48.

Goldberg RI, Smith RM, Jarrett L. 1987. Insulin and α_2-macroglobulin-methylamine undergo endocytosis by different mechanisms in rat adipocytes: I. Comparison of cell surface events. J Cell Physiol 133:203–212.

Heider JG, Boyett RL. 1978. The picomole determination of free and total cholesterol in cells in culture. J Lipid Res 19:514–518.

Jordana X, Allende CC, Allende JE. 1981. Guanine nucleotides are required for progesterone inhibition of amphibian oocyte adenylate cyclase. Biochem Int 3:527–532.

Laemmli U. 1970. Cleavage of structural proteins during the assembly of the head of bacteriophage T4. Nature 227:680–685.

Maller JL. 1985. Regulation of amphibian oocyte maturation. Cell Differ 16:211–221.

Maller JL, Koontz JW. 1981. A study of the induction of cell division in amphibian oocytes by insulin. Dev Biol 85: 309–316.

Maller JL, Krebs EG. 1980. Regulation of oocyte maturation. Curr Topics Cell Regul 16:271–311.

Masui Y. 1967. Relative roles of the pituitary, follicle cells, and progesterone in the induction of oocyte maturation in *Rana pipiens*. J Exp Zool 166:365–376.

Mineo C, James GL, Smart EJ, Anderson RGW. 1996. Localization of epidermal growth-factor-stimulated Ras/Raf-1 interaction to caveolae membrane. J Biol Chem 271:11930–11935.

Morrill GA, Kostellow AB. 1999. Progesterone induces meiotic division in the amphibian oocyte by releasing lipid second messengers from the plasma membrane. Steroids 64:157–167.

Morrill GA, Doi K, Kostellow AB. 1989. Progesterone induces transient changes in plasma membrane fluidity of amphibian oocytes during the first meiotic division. Arch Biochem Biophys 269:690–694.

Morrill GA, Doi K, Erlichman J, Kostellow AB. 1993. Cyclic AMP binding to the amphibian oocyte plasma membrane: possible interrelationship between meiotic arrest and membrane fluidity. Biochim Biophys Acta 1158:146–154.

Morrill GA, Ma GY, Kostellow AB. 1994. Progesterone-induced phospholipid N-methylation and sphingomyelin synthesis in the amphibian oocyte plasma membrane: a second source of the 1,2-diacylglycerol second messenger associated with the G2/M transition. Biochim Biophys Acta 1224:589–596.

Okamoto T, Schlegal A, Scherer PE, Lisanti MP. 1998. Caveolins, a family of scaffolding proteins for organizing "preassembled signaling complexes" at the plasma membrane. J Biol Chem 273:5419–5422.

Rothberg KG, Heuser JE, Donzell WC, Ying Y-S, Glenney JR, Anderson RGW. 1992. Caveolin, a protein of caveolae membrane coats. Cell 68:673–682.

Sadler SE. 1991a. Type III phosphodiesterase plays a necessary role in the growth-promoting actions of insulin, insulin-like growth factor-1, and Ha p21*ras* in *Xenopus laevis* oocytes. Mol Endocrinol 5:1939–1946.

Sadler SE. 1991b. Inhibitors of phosphodiesterase III block stimulation of *Xenopus laevis* oocyte ribosomal S6 kinase activity by insulin-like growth factor-1. Mol Endocrinol 5:1947–1954.

Sadler SE. 2000. Membrane-associated Ras is enriched in low-density caveolae-like membrane from *Xenopus laevis*oocytes. Mol Biol Cell 11:53a.

Sadler SE, Maller JL. 1981. Progesterone inhibits adenylate cyclase in *Xenopus* oocytes. Action on the guanine nucleotide regulatory protein. J Biol Chem 256:6368–6373.

Sadler SE, Maller JL. 1983. Inhibition of *Xenopus* oocyte adenylate cyclase by progesterone and 2′,5′-dideoxyadenosine is associated with slowing of guanine nucleotide exchange. J Biol Chem 258:7935–7941.

Sadler SE, Maller JL. 1987. In vivo regulation of cyclic AMP phosphodiesterase in *Xenopus* oocytes. Stimulation by insulin and insulin-like growth factor 1. J Biol Chem 262:10644–10650.

Sathananthan AH. 1997. Ultrastructure of the human egg. Hum Cell 10:21–38.

Scherer PE, Okamoto T, Chun M, Nishimoto I, Lodish HF, Lisanti MP. 1996. Purification, sequence, and expression of caveolin-2 defines the caveolin gene family. Proc Natl Acad Sci 93:131–135.

Smart EJ, Ying Y-S, Anderson RGW. 1995. Hormonal regulation of caveolae internalization. J Cell Biol 131: 929–938.

Smith LD. 1989. The induction of oocyte maturation: transmembrane signaling events and regulation of the cell cycle. Development 107:685–699.

Smith RM, Jarrett L. 1988. Receptor-mediated endocytosis and intracellular processing of insulin: ultrastructural and biochemical evidence for cell-specific heterogeneity and distinction from nonhormonal ligands. Lab Invest 58:613–629.

Smith RM, Jarrett L. 1990. Differences in adenosine triphosphate dependency of receptor-mediated endocytosis of α_2-macroglobulin and insulin correlate with separate routes of ligand-receptor complex internalization. Endocrinology 126:1551–1560.

Song KS, Li S, Okamoto T, Quilliam LA, Sargiacomo M, Lisanti MP. 1996a. Co-purification and direct interaction of Ras with caveolin, an integral membrane protein of caveolae microdomains. Detergent-free purification of caveolae membranes. J Biol Chem 271:9690–9697.

Song KS, Scherer PE, Tang ZL, Okamoto T, Li S, Chafel M, Chu C, Kohtz DS, Lisanti MP. 1996b. Expression of caveolin-3 in skeletal, cardiac, and smooth muscle cells. Caveolin-3 is a component of the sarcolemma and co-fractionates with dystrophin and dystrophin-associated glycoproteins. J Biol Chem 271:15160–15165.

Stan R-V, Roberts WG, Predescu D, Ihida K, Saucan L, Ghitescu L, Palade GE. 1997. Immunoisolation and partial characterization of endothelial plasmalemmal vesicles (caveolae). Mol Biol Cell 8:595–605.

Strum JC, Swenson KI, Turner JE, Bell RM. 1995. Ceramide triggers meiotic cell cycle progression in *Xenopus* oocytes. A potential mediator of progesterone-induced maturation. J Biol Chem 270:13541–13547.

Taghon MS, Sadler SE. 1994. Insulin-like growth factor 1 receptor-mediated endocytosis in *Xenopus laevis* oocytes. Dev Biol 163:66–74.

Tang ZL, Scherer PE, Okamoto T, Song K, Chu C, Kohtz DS, Nishimoto I, Lodish HF, Lisanti MP. 1996. Molecular cloning of caveolin-3, a novel member of the caveolin gene family expressed predominately in muscle. J Biol Chem 271:2255–2261.

Wu C, Butz X, Ying Y-S, Anderson RGW. 1997. Tyrosine kinase receptors concentrated in caveolae-like domains from neuronal plasma membrane. J Biol Chem 272: 3554–3559.

Yamada E. 1955. The fine structure of the gall bladder epithelium of the mouse. J Biophys Biochem Cytol 1: 445–458.